© 2015. Published by The Company of Biologists Ltd | Journal of Cell Science (2015) 128, 3277-3289 doi:10.1242/jcs.170878

RESEARCH ARTICLE

Centrosomal AKAP350 and CIP4 act in concert to define the polarized localization of the centrosome and Golgi in migratory cells

Facundo M. Tonucci[1], Florencia Hidalgo[1], Anabela Ferretti[1], Evangelina Almada[1], Cristián Favre[1], James R. Goldenring[2,3], Irina Kaverina[3], Arlinet Kierbel[4] and M. Cecilia Larocca[1,*]

ABSTRACT

The acquisition of a migratory phenotype is central in processes as diverse as embryo differentiation and tumor metastasis. An early event in this phenomenon is the generation of a nucleus–centrosome–Golgi back-to-front axis. AKAP350 (also known as AKAP9) is a Golgi and centrosome scaffold protein that is involved in microtubule nucleation. AKAP350 interacts with CIP4 (also known as TRIP10), a cdc42 effector that regulates actin dynamics. The present study aimed to characterize the participation of centrosomal AKAP350 in the acquisition of migratory polarity, and the involvement of CIP4 in the pathway. The decrease in total or in centrosomal AKAP350 led to decreased formation of the nucleus–centrosome–Golgi axis and defective cell migration. CIP4 localized at the centrosome, which was enhanced in migratory cells, but inhibited in cells with decreased centrosomal AKAP350. A decrease in the CIP4 expression or inhibition of the CIP4–AKAP350 interaction also led to defective cell polarization. Centrosome positioning, but not nuclear movement, was affected by loss of CIP4 or AKAP350 function. Our results support a model in which AKAP350 recruits CIP4 to the centrosome, providing a centrosomal scaffold to integrate microtubule and actin dynamics, thus enabling centrosome polarization and ensuring cell migration directionality.

KEY WORDS: AKAP350, AKAP450, CIP4, Centrosome, Actin, Migratory polarity

INTRODUCTION

In vivo migration of mammalian cells is a complex phenomenon that is highly relevant to a wide range of physiological processes, such as embryogenesis, wound healing, homing of lymphocytes to lymphoid organs and for defense against infections, and to pathological processes such as tumor progression (Trinkaus, 1984). The first process required for directional cell migration is the asymmetric reorganization of the cell components in order to acquire a front–rear polarity. In most cell types, during the acquisition of migratory polarity, the nucleus moves to the back, whereas the centrosome and Golgi complex relocate to the front of the cell. This polarized organization ensures the directional trafficking of membranes and regulatory proteins towards the leading edge (Yadav et al., 2009; Etienne-Manneville, 2013). In non-polarized cells, the centrosomes are anchored to the nucleus through microtubules and actin fibers, and the Golgi is positioned close to the centrosomes (Sutterlin and Colanzi, 2010). Cdc42 activation at the front of the cell is the earliest cell event presently identified that leads to the centrosome and Golgi relocation in migratory cells. The most-accepted model for the organization of the nucleus–centrosome–Golgi axis in migratory cells is that cdc42 activation at the leading edge leads to the association of specific proteins with the microtubule plus end, as well as dynein recruitment and anchoring at this position, thus leading to microtubule pulling and centrosome localization in front of the nucleus (Etienne-Manneville, 2013). Studies in migratory fibroblasts suggest that, upon cdc42 activation at the front of the cell, the nucleus moves backwards, whereas the centrosome is kept in its central position by a dynein- and microtubule-dependent process (Gomes et al., 2005). Both the factors governing the centrosome positioning relative to the nucleus and the centrosomal players in the reorientation of this organelle are still unclear.

AKAP350 (also known as AKAP450, CG-NAP or AKAP9) is an A-kinase anchoring protein (Schmidt et al., 1999), which represents an excellent centrosomal candidate to organize this organelle relocation during cell migration. AKAP350 contains a C-terminal centrosome-targeting domain, i.e. the PACT domain (Gillingham and Munro, 2000) and two Golgi-targeting domains (Shanks et al., 2002; Hurtado et al., 2011), which enable AKAP350 positioning at these organelles. The involvement of centrosomal AKAP350 in cell migration was first suggested after studies in T cells, which demonstrated that the overexpression of the centrosome-targeting domain of AKAP350 leads to inhibition of the integrin-induced-cell migration (El Din El Homasany et al., 2005). More recent studies have confirmed that AKAP350 participates in cell migration in immortalized epithelial cells (Rivero et al., 2009). Furthermore, expression of the *AKAP350* gene is upregulated in metastatic melanoma cells, and this protein expression is essential for melanoma cell migration (Kabbarah et al., 2010). Nevertheless, the mechanisms involved in promoting migration have not been elucidated. AKAP350 has been proposed to recruit the γ-tubulin-containing ring (γ-TURC) proteins GCP2 and GCP3, thus participating in microtubule nucleation at the centrosomes and at the Golgi complex (Takahashi et al., 2002; Larocca et al., 2006; Rivero et al., 2009). Considering that Golgi-derived microtubules are necessary for directional migration (Efimov et al., 2007), it has been suggested that, by nucleating microtubules at the Golgi, AKAP350 enables the polarized trafficking of membranes and proteins towards the leading edge (Rivero et al., 2009). In terms of

[1]Instituto de Fisiología Experimental, Consejo de Investigaciones Científicas y Técnicas, Facultad de Ciencias Bioquímicas y Farmacéuticas, Universidad Nacional de Rosario, Rosario 2000, Argentina. [2]Department of Surgery, Epithelial Biology Center, Vanderbilt University School of Medicine, Vanderbilt-Ingram Cancer Center and the Nashville VA Medical Center, Nashville, TN 37232, USA. [3]Department of Cell and Developmental Biology, Epithelial Biology Center, Vanderbilt University School of Medicine, Vanderbilt-Ingram Cancer Center and the Nashville VA Medical Center, Nashville, TN 37232, USA. [4]Instituto de Investigaciones Biotecnológicas Dr. Rodolfo A. Ugalde (IIB-INTECH), Universidad Nacional de San Martín, Consejo Nacional de Investigaciones Científicas y Técnicas (UNSAM-CONICET), San Martín 1650, Buenos Aires, Argentina.

*Author for correspondence (larocca@ifise-conicet.gov.ar)

Received 27 February 2015; Accepted 17 July 2015

Journal of Cell Science (2015) 128, 3277-3289 doi:10.1242/jcs.170878

Golgi and centrosomal reorientation towards the leading edge, which is an earlier event, Rivero et al. (2009) report that they are unaffected by the decrease in AKAP350 expression. Nevertheless, subsequent studies from the same group indicate that overexpression of the N-terminal Golgi-targeting domain of AKAP350 inhibits both centrosome and Golgi reorientation towards the leading edge (Hurtado et al., 2011). The participation of centrosomal AKAP350 in these events has not been addressed so far.

The cdc42-interacting protein 4 (CIP4; also known as TRIP10) is a candidate partner for AKAP350 in the scenario of directional cell migration (Larocca et al., 2004). CIP4 is an effector protein of cdc42 (Aspenström, 1997). Structurally, CIP4 belongs to the family of F-BAR proteins. This is a group of proteins characterized by an N-terminal Fes-CIP4 homology domain followed by a coiled-coil domain (F-BAR domain), which interact with negatively charged membrane phospholipids, thus modulating membrane curvature (Roberts-Galbraith and Gould, 2010). This domain is also responsible for CIP4 association with microtubules and AKAP350 (Tian et al., 2000; Larocca et al., 2004). CIP4 also contains a C-terminal SH3 domain, which mediates CIP4 interactions with numerous proteins – including dynamin-2 (Tsujita et al., 2006), and the regulators of actin nucleation WASP and formin DAAM1 (Tian et al., 2000; Aspenström et al., 2006). Therefore, CIP4 acts downstream of cdc42 activation to promote membrane deformation, vesicle scission and actin polymerization (Fricke et al., 2009), thus participating in endocytosis (Leibfried et al., 2008; Hartig et al., 2009; Feng et al., 2010), and in the formation of lamellapodial protrusions (Saengsawang et al., 2012) and pro-invasive invadopodia structures (Pichot et al., 2010; Hu et al., 2011). Regarding cell migration, CIP4 is upregulated during epithelial–mesenchymal transition (Zhang et al., 2013) and has been reported to be essential for the development of metastatic properties in different types of cancer cells (Pichot et al., 2010; Truesdell et al., 2014; Rolland et al., 2014; Koshkina et al., 2013). Although most studies point to its involvement in the formation of membrane structures that are necessary for cell migration, the actual mechanism by which CIP4 plays a central role in the acquisition of migratory properties has not been clarified yet. CIP4 is also involved in non-membranous processes. Studies performed in natural killer cells show that CIP4 localizes to the centrosome during cell activation, where it functions downstream of cdc42 activation to promote centrosome relocation to the immune synapse (Banerjee et al., 2007). CIP4 localization at this non-membranous organelle in non-immune cells has not been characterized yet.

The major aim of this study was to gain insight into the centrosomal mechanisms governing centrosome repositioning towards the leading edge during directional cell migration. We found that CIP4 localizes at the centrosome in an AKAP350-dependent manner and that this localization is increased in migrating cells. Furthermore, we demonstrated that loss of centrosomal AKAP350 leads to defective directional cell migration, which correlates with decreased polarization of the centrosome and Golgi within the cell, and that this phenotype is mimicked upon knockdown of CIP4 expression or through the inhibition of the interaction of CIP4 with AKAP350.

RESULTS

Centrosomal AKAP350 contributes to directional cell migration

We first analyzed the participation of centrosomal AKAP350 in the directional migration of hepatocarcinoma-derived cells HepG2. We used a HepG2 cell line that constitutively expressed the AKAP350 centrosome-targeting domain (AKAP350CTD), which consequently exhibits a 50% decrease in the centrosomal localization of endogenous AKAP350 (Mattaloni et al., 2013). We generated experimental wounds and analyzed wound closure after 24 and 48 h. After 48 h, the area corresponding to the wound was significantly larger in AKAP350CTD cells (Fig. 1A). In order to develop a more sensitive method for quantifying the efficiency of cell migration, which was not dependent on the rate of cell proliferation, we adopted a different assay. We performed experimental wounding assays using a mixed population of cells that contained equal numbers of AKAP350CTD and control cells. After different periods of time, we calculated the ratio for each group

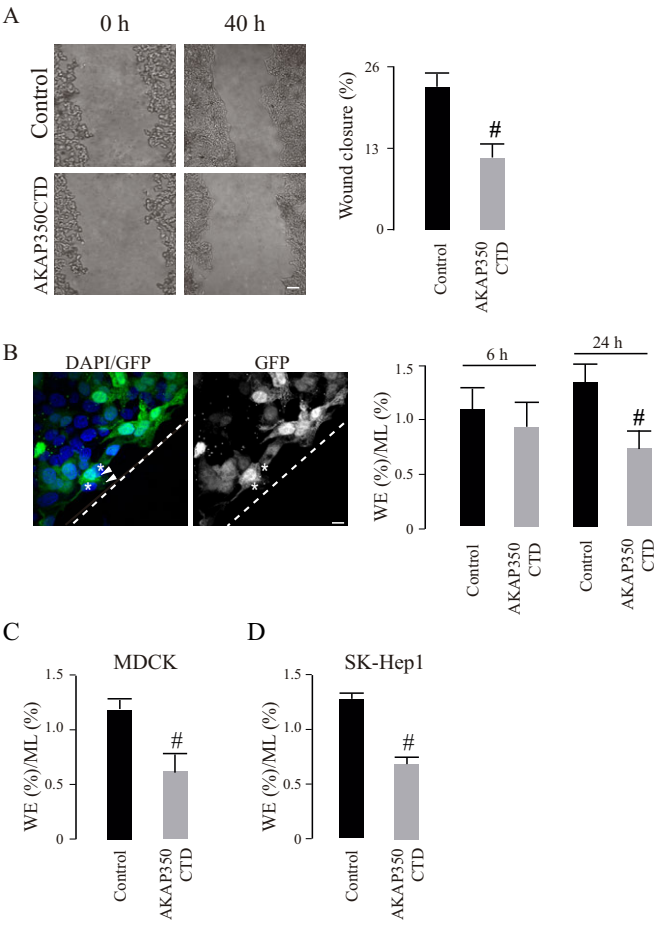

Fig. 1. Participation of centrosomal AKAP350 in cell migration. (A) HepG2 cells stably expressing EGFP (control) or EGFP–AKAP350CTD (AKAP350CTD) were grown to confluence and subjected to scratch wounding (t0). Phase contrast images illustrate wound gaps at 0 h and 40 h. The bar graph represents the average difference between gap areas from the same field at 0 h and 40 h, expressed as a percentage of the initial gap area. (B–D) Equal amounts of HepG2, MDCK or SK-Hep1 control and AKAP350CTD cells were mixed, and wound healing assays were performed. Cells were fixed at 6 h and 24 h (HepG2), at 5 h (MDCK) or at 3 h (SK-Hep1) and stained with DAPI; images were then analyzed by using confocal microscopy. The quantity of control and AKAP350CTD cells at the wound edge (WE) and in the unperturbed confluent monolayer (ML) were determined. The image shows HepG2 cell distribution at the wound edge at 24 h (B). The bar graph represents the average ratio between the percentages of cells in both locations for HepG2 (B), MDCK (C) and SK-Hep1 (D) cells. Data are expressed as means±s.e.m. of at least eight fields (A) or 150 cells distributed in six separate fields corresponding either to the WE or the ML (B–D), representative of four (A), five (B) or three (C,D) independent experiments Dashed lines indicate the wound direction. Asterisks indicate AKAP350CTD cells at the wound edge, whereas arrowheads specify AKAP350CTD expression at the centrosomes in these cells. $^{\#}P<0.05$. Scale bars: 200 µm (A); 10 µm (B).

Journal of Cell Science (2015) 128, 3277-3289 doi:10.1242/jcs.170878

of cells at the wound edge, and related it to the ratio of cells in the monolayer. Our results indicated that, 24 h after the wound was generated, control cells had a migratory advantage over the AKAP350CTD cells (Fig. 1B). We verified the relevance of these findings using two different cell lines that migrate more efficiently – MDCK cells, derived from normal epithelia; and SK-Hep1 cells, which are derived from endothelial hepatic tumor cells (Fig. 1C,D). AKAP350CTD expression also impaired migration of these cells, which was already evident 3 h after the experimental wound was generated.

Centrosomal AKAP350 participates in the polarization of the centrosome and Golgi towards the wound edge

The positioning of the centrosome and the Golgi in front of the nucleus is a common feature at the early stages of acquisition of the cell migratory phenotype. We analyzed the involvement of centrosomal AKAP350 in this process at two different time points – at 6 h, when there is still no evident difference in the migration of HepG2 AKAP350CTD cells; and at 24 h after wounding. In both cases, we observed that HepG2 AKAP350CTD cells showed a significant inhibition of the polarization of the centrosome and Golgi within the cell (Fig. 2A). The same analysis performed at earlier time points in MDCK and in SK-Hep1 cells led to similar conclusions (Fig. 2B,C).

The Golgi dynamics are crucial for centrosome repositioning in migrating cells (Sutterlin and Colanzi, 2010). We examined whether the AKAP350CTD-induced impairment in centrosome and Golgi repositioning was related to a direct effect of the expression of this domain on the Golgi integrity (Fig. 3). Previous studies have indicated that there is a Golgi-targeting domain located upstream of the centrosome-targeting domain in the AKAP350 amino acid sequence (Shanks et al., 2002). Our previous studies indicate that a decrease in AKAP350 expression leads to Golgi unstacking and vesiculation (Larocca et al., 2004). Thus, we first analyzed the Golgi levels of AKAP350 in AKAP350CTD cells. We found that the percentage of AKAP350 present at the Golgi apparatus did not differ between AKAP350CTD and control cells (Fig. 3A). The total levels of AKAP350, as analyzed by western blotting, were similar in both groups of cells (data not shown). Considering that GM130 is an AKAP350 partner (Rivero et al., 2009), which is directly involved

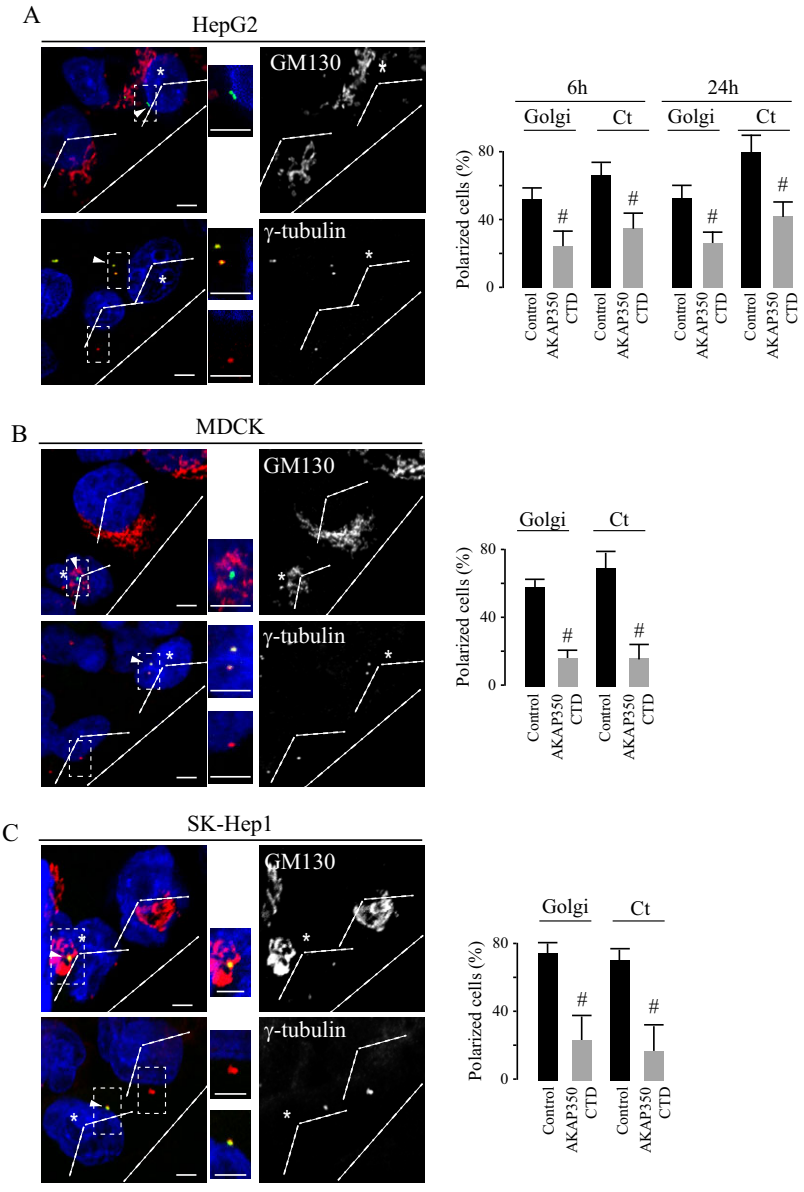

Fig. 2. Participation of centrosomal AKAP350 in Golgi and centrosome polarization during cell migration. HepG2, SK-Hep1 and MDCK AKAP350CTD cells were mixed with an equal number of non-transfected (control) cells and seeded, and wound healing assays were performed. Cells were fixed 6 h and 24 h (A, HepG2) or 2 h (B, MDCK; C, Sk-Hep1) after scratch wounding, and stained with anti-GM130 and anti-γ tubulin antibodies for Golgi and centrosome visualization, respectively. Merged images (left) show DAPI in blue, and GM130 or γ-tubulin in red, and AKAP350CTD expression in green. Single-channel images are shown on the right. Regular dashed lines (––) indicate the 120° angle facing the wound, which delimitates the anterior pole of the cell, and irregular dashed lines indicate the direction of the wound (-·-). The inset images show magnified views of the centrosomes (boxed areas). Those cells with more than 50% of their Golgi at the anterior pole were considered polarized. Centrosomes were counted as polarized when they were localized at the anterior pole. Asterisks specify AKAP350CTD cells, whereas arrowheads indicate AKAP350CTD expression at the centrosomes in these cells. Bar graphs show the percentage of cells with polarized Golgi or centrosomes (Ct). Data are expressed as means± s.e.m. of at least 40 cells, representative of three independent experiments. $^{\#}P<0.05$. Scale bars: 5 µm.

Journal of Cell Science (2015) 128, 3277-3289 doi:10.1242/jcs.170878

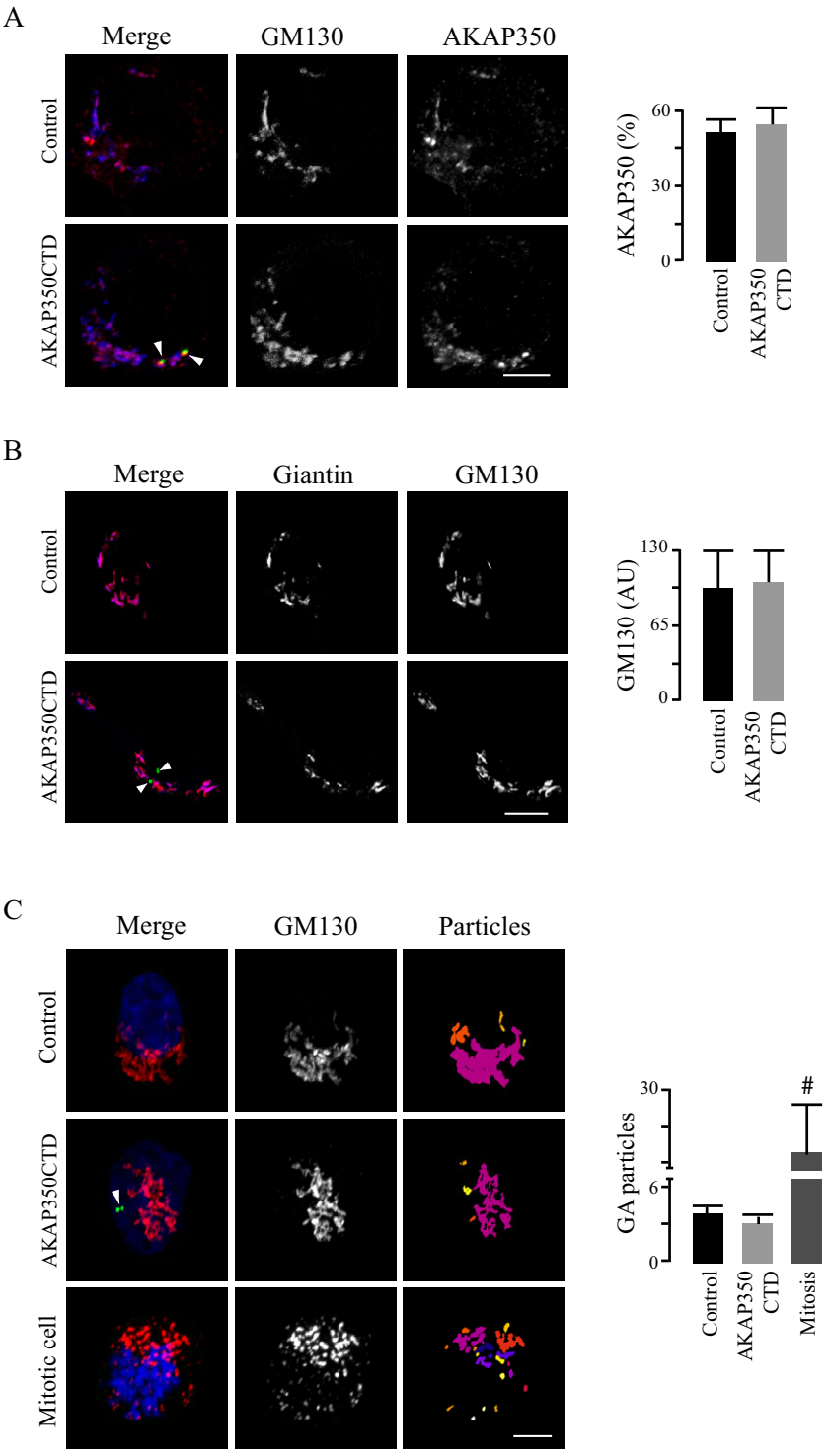

Fig. 3. The Golgi complex in AKAP350CTD cells. Control and AKAP350CTD cells were mixed, grown to confluence, fixed and stained with DAPI, anti-GM130 and anti-AKAP350 or anti-giantin antibodies. Images were obtained by using confocal microscopy and analyzed using ImageJ tools. Comparisons were performed by pairing cells within the same field. (A) Merged images show AKAP350CTD expression (green), and staining of AKAP350 (red) and GM130 (blue). AKAP350 fluorescence corresponding to the Golgi was established by delimiting its volume with a GM130 mask. Bar graphs show the density of AKAP350 fluorescence corresponding to the Golgi complex expressed as percentage of the total cell fluorescence. (B) Merged images show AKAP350CTD expression (green), and staining of GM130 (red) and giantin (blue). Bar graphs show the density of GM130 fluorescence corresponding to the Golgi, the volume of which was delimited using a giantin mask. (C) Merged images show AKAP350CTD expression (green), and staining of GM130 (red) and DNA (DAPI, blue). Golgi architecture was analyzed by using the ImageJ 3D object counter plugin. The third column shows the *z*-projection of the differentially colored Golgi-complex (GA) particles. Bar graphs shown the number of Golgi particles per cell for each group of cells. Mitotic cells, identified by using their chromosomal morphology, were used as a methodological control. Arrowheads indicate centrosomal AKAP350CTD expression. Data are expressed as means±s.e.m. of at least 40 cells, representative of three independent experiments. $^{\#}P<0.01$. AU, arbitrary units. Scale bars: 5 µm.

in centrosomal reorientation (Kodani and Sütterlin, 2008), we further analyzed the Golgi levels of this protein. Our results indicated that GM130 levels at the Golgi were unaffected by the expression of the AKAP350CTD domain (Fig. 3B). The participation of centrosomal microtubules in Golgi organization has been well characterized (Vinogradova et al., 2012). Bearing in mind that AKAP350 is involved in the centrosomal nucleation and stabilization of microtubules (Larocca et al., 2006), we analyzed the Golgi architecture in AKAP350CTD cells. We automatically selected GM130-positive particles in control and AKAP350CTD cells by using the ImageJ 3D object counter. We analyzed mitotic cells, which fragment their Golgi in order to divide, as a control. The analysis of the Golgi architecture showed that the Golgi stacking was preserved in AKAP350CTD cells (Fig. 3B). Thus, these results suggest that the defective cell polarization and migration observed in AKAP350CTD cells was not due to a primary effect on the structure of the Golgi complex.

To confirm whether the impairment of centrosomal and Golgi polarization was due to a decrease in AKAP350 function, we analyzed centrosome and Golgi polarization in AKAP350

Journal of Cell Science (2015) 128, 3277-3289 doi:10.1242/jcs.170878

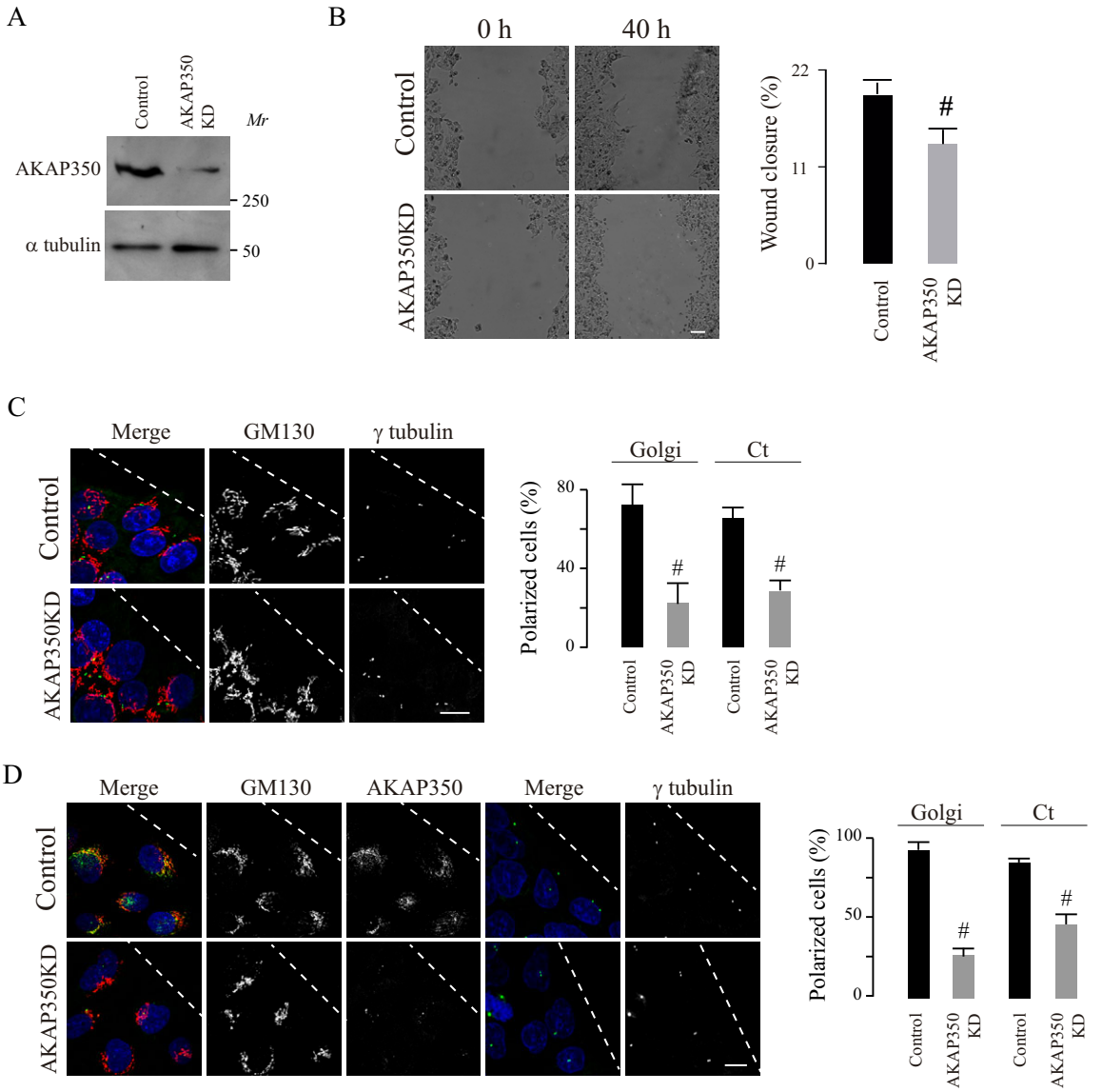

Fig. 4. Centrosome and Golgi polarity in AKAP350KD cells. AKAP350KD HepG2 and MDCK cells were generated as described in Materials and Methods, and the decrease in AKAP350 expression was verified by immunoblotting and immunofluorescence analyses. Control cells expressing non-specific siRNAs [or small hairpin (sh)RNAs] and AKAP350KD cells were seeded, and wound healing assays were performed. (A) Immunoblots showing AKAP350 expression in control and AKAP350KD HepG2 cells, and the corresponding loading control. (B) Phase contrast images illustrate wound gaps at 0 h and 40 h. Bar graphs show the average difference between gap areas from the same field at 0 h and 40 h, expressed as a percentage of the initial gap area. (C) HepG2 cells were fixed 6 h after scratch wounding. Merged images show nuclear (blue), γ-tubulin (green) and GM130 (red) staining in HepG2 cells at the wound edge. (D) MDCK cells were fixed 2 h after scratch wounding. Merged images show nuclear (blue), GM130 (red, first column) and AKAP350 (green, first column) or γ-tubulin (green, fourth column) staining in MDCK cells at the wound edge. Bar graphs show the percentage of cells with polarized Golgi or centrosomes. Data are expressed as means±s.e.m. of at least eight fields (B) or 40 cells, representative of four (C) or three (B,D) independent experiments. Dashed lines indicate the direction of the wound. Means±s.e.m.; $^{\#}P<0.05$. Ct, centrosomes. Scale bars: 5 µm.

knockdown (AKAP350KD) cells. We prepared HepG2 AKAP350KD cells, as we have previously described (Mattaloni et al., 2012), and first evaluated the impact of the decrease in AKAP350 expression on HepG2 cell migration in wound healing assays. We then verified that, as previously described in melanoma cells, the cell migration efficiency of HepG2 AKAP350KD cells was impaired (Fig. 4B). The analysis of centrosome and Golgi polarity in these cells showed that the decrease in AKAP350 expression (Fig. 4C) led to a phenotype similar to that observed in AKAP350CTD cells (Fig. 2). To verify that this was not a peculiarity of HepG2 cells, we generated MDCK AKAP350KD cells, as described in the Materials and Methods. The analysis of centrosome and Golgi polarity in these cells was in accordance with our observations in HepG2 cells (Fig. 4D), thus confirming the participation of AKAP350 in the polarization of the centrosome and Golgi within the cell towards the wound edge. The phenotype of AKAP350KD cells on that regard was confirmed using a second siRNA or shRNA in HepG2 and MDCK cells, respectively (not shown).

AKAP350 recruits CIP4 to the centrosome in migrating cells

CIP4 is predominantly recognized as a membrane–actin-cytoskeleton linker, involved in the modulation of membrane curvature. Immunofluorescence studies in natural killer cells show that, during the interaction with target cells, CIP4 colocalizes with centrosomal markers (Banerjee et al., 2007). Hence, we investigated CIP4 localization at the centrosomes in HepG2 cells. Subcellular

Journal of Cell Science (2015) 128, 3277-3289 doi:10.1242/jcs.170878

fractions enriched for centrosomes were prepared by using differential centrifugation on a discontinuous sucrose gradient. The purity of this fraction was verified through the presence of the centrosomal protein γ-tubulin and the absence of Rab11, which is a marker of the pericentrosomal apical recycling compartment (Fig. 5A). We found that CIP4 was present in the fraction that contained the centrosomes. Estimates that considered the total protein recovery and CIP4 band density for each fraction indicated that approximately 4% of total CIP4 localized at the centrosome. We further analyzed CIP4 localization at the centrosome by using confocal microscopy. In accordance with the biochemical results, CIP4 colocalized with γ-tubulin at this organelle (Fig. 5B). By contrast, the Golgi protein GM130, which was positioned very close to the centrosome in some cells, did not colocalize with the centrosomal marker, thus confirming the specificity of CIP4 and γ-tubulin colocalization (Fig. 5B). It is noteworthy that not every cell growing in the monolayer contained CIP4-positive centrosomes. Interestingly, the differential quantitative analysis of CIP4 localization in cells at the wound edge versus cells in the monolayer indicated that migrating cells had increased levels of

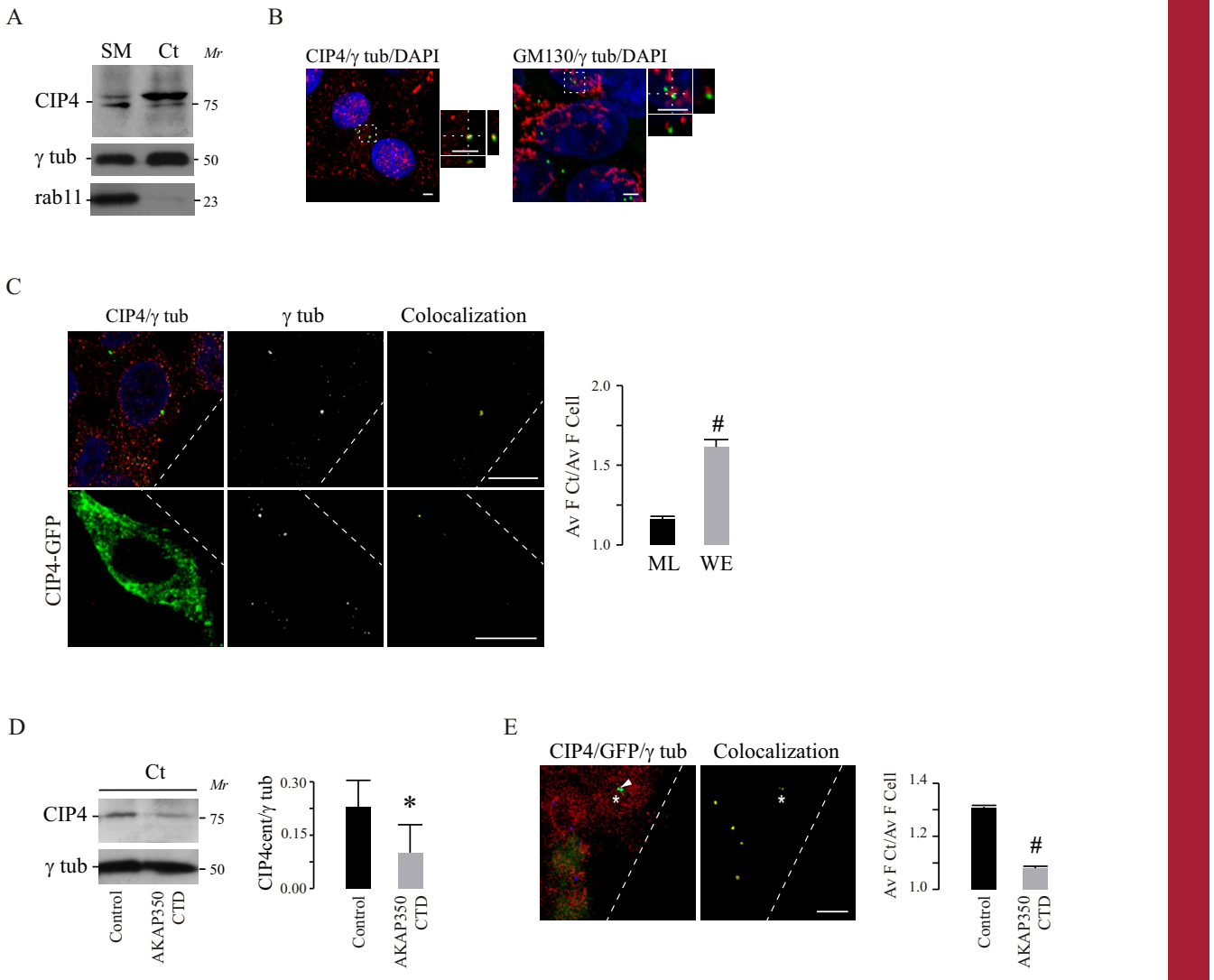

Fig. 5. Centrosomal localization of CIP4. (A) Cell lysates were subjected to differential centrifugation using a sucrose gradient as described in Materials and Methods. The centrosomal fraction (Ct) was analyzed next to the starting material (SM) for CIP4 expression by western blotting. Centrosome enrichment was verified by γ-tubulin (γ tub) immunoblot analysis. Rab11 immunoblotting was used to rule out cross-contamination with cell pericentrosomal membranes. (B) Merged images show the visualization of CIP4 (red), γ-tubulin (green) and DAPI staining in HepG2 cells. The smaller panels at the right of each of the larger images show magnified views of the centrosome (boxed area), with the corresponding *x*,*z* and *x*,*y* projections. (C) HepG2 cells and HepG2 cells transiently expressing CIP4–GFP were subjected to wound healing assays, and fixed 6 h after scratch wounding. The merged images show the visualization of CIP4 (red), γ-tubulin (green), in the first row; or CIP4–GFP expression (green), γ-tubulin (red), in the second row; and DAPI staining in cells at the wound edge. The third-column images illustrate CIP4 colocalization with γ-tubulin (yellow). Bar graphs represent the ratio of the average endogenous CIP4 intensity of fluorescence (Av F) at the centrosome relative to the complete cell at the wound edge (WE) and at the intact monolayer (ML), representative of three independent experiments. (D) Immunoblotting of centrosome-enriched fractions of control and AKAP350CTD cells. Bar graphs represent the average density of the band corresponding to centrosomal CIP4 relative to γ-tubulin of three independent experiments. (E) Equal amounts of HepG2 control and AKAP350CTD cells were mixed, and wound healing assays were performed. Cells were fixed 6 h after scratch wounding. The merged image shows the visualization of CIP4 (red), γ-tubulin (blue) staining, and GFP–AKAP350CTD expression (green). Bar graphs show the ratio of average CIP4 intensity at the centrosome relative to the complete cell in AKAP350CTD and control cells, representative of three experiments. Arrowheads indicate AKAP350CTD expression at the centrosome. Asterisks indicate AKAP350CTD cells. Scale bars: 3 µm (B); 10 µm (C,E). Data are expressed as means±s.e.m. of at least 40 (C) or 20 (D) cells. $^{\#}P<0.05$.

Journal of Cell Science (2015) 128, 3277-3289 doi:10.1242/jcs.170878

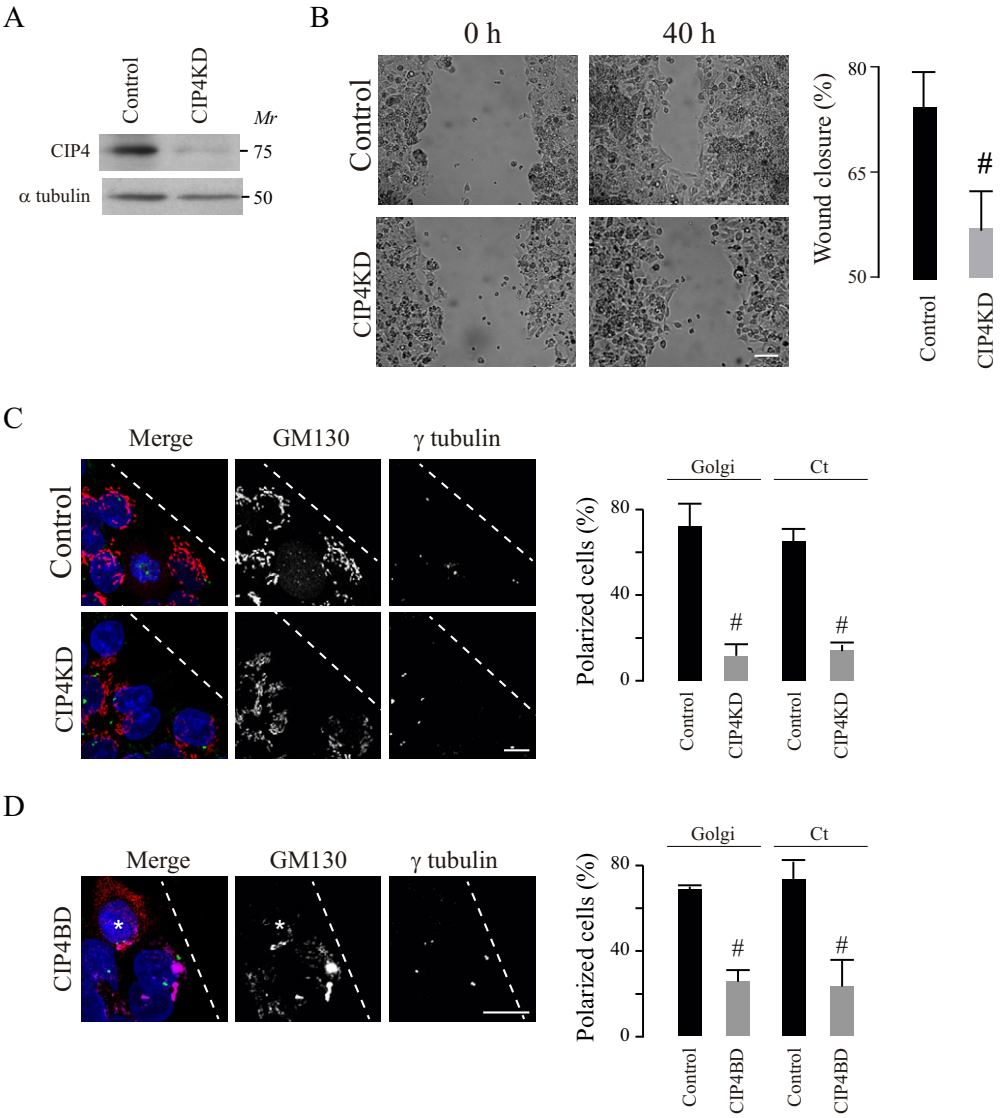

Fig. 6. CIP4 participation in Golgi and centrosome polarization during cell migration. CIP4KD cells were generated as described in Materials and Methods. Control and CIP4KD cells were seeded, and wound healing assays were performed. (A) Immunoblotting analysis of CIP4 expression in control and CIP4KD cells, and the corresponding loading control. (B) Phase contrast images illustrate wound gaps at 0 h and 40 h. Bar graphs show the average difference between the gap areas from the same field at 0 h and 40 h, expressed as a percentage of the initial gap area. (C) Images show GM130 and γ-tubulin staining in HepG2 cells at the wound edge (dashed lines). Relevance of the CIP4–AKAP350 interaction. (D) Cells with transient expression of the minimal AKAP350 domain responsible for its interaction with CIP4 bound to m-Cherry (CIP4BD) were generated and subjected to wound healing assays. The merged image shows staining of GM130 (magenta), γ-tubulin (green) and the nucleus (DAPI, blue), and CIP4BD expression (red) in cells at the wound edge (dashed line). Asterisks indicate transfected cells. Bar graphs illustrate the percentage of cells with polarized Golgi or centrosome (Ct) distribution. Data are expressed as means±s.e.m. of at least eight fields (B) or 40 cells (C,D), representative of three independent experiments. $^{\#}P<0.05$. Scale bars: 50 μm (B) or 10 μm (C,D).

CIP4 at the centrosomes (Fig. 5C, first row). In order to verify the specificity of these results, we generated cells that expressed CIP4 fused to green fluorescent protein (GFP) at its C-terminal domain (CIP4–GFP) and analyzed the centrosomal expression of this fusion protein. Similar to the endogenous protein, CIP4–GFP colocalized with centrosomal γ-tubulin, and this colocalization was more prominent in cells at the wound edge (Fig. 5C, second row). Considering that CIP4 interacts with AKAP350 (Larocca et al., 2004), we evaluated the centrosomal localization of CIP4 in cells in which AKAP350 had delocalized from this organelle. Using the biochemical assay, we found that AKAP350CTD cells exhibited a 50% decrease in centrosomal CIP4 (Fig. 5D), indicating that centrosomal localization of CIP4 is AKAP350 dependent. These results were corroborated by using quantitative confocal microscopy to study the colocalization of CIP4 with γ-tubulin in a mixed population of AKAP350CTD and control cells (Fig. 5E). Similar results were obtained in SK-Hep1 cells (data not shown).

CIP4 and its interaction with AKAP350 are essential for centrosome and Golgi polarization

In order to evaluate CIP4 participation in the positioning of the centrosome and Golgi at the front pole of the cell, we generated HepG2 cells that had decreased CIP4 expression (CIP4KD), by using RNA interference. The CIP4KD cells showed an approximate 85% decrease in CIP4 expression, as verified by western blotting (Fig. 6A). Next, we evaluated wound closure, and centrosome and Golgi polarity in CIP4KD cells at the wound edge. We found that the decrease in CIP4 expression decreased cell migration efficiency (Fig. 6B) and induced a significant reduction (−75%) in the fraction of cells that exhibited a polarized phenotype, thus demonstrating CIP4 participation in this process (Fig. 6C). Considering that CIP4 is involved in several processes related to cell migration, including the disassembly of the adherens junctions (Rolland et al., 2014), the mechanism involved in centrosome and Golgi polarization could be independent of the interaction of CIP4 with AKAP350. Therefore, we evaluated whether this interaction was relevant for centrosomal and Golgi polarization. We engineered cells in which the AKAP350–CIP4 interaction was competitively inhibited through the expression of the minimal AKAP350 domain that is responsible for the interaction with CIP4 [AKAP350(1076–2143); referred to as CIP4BD] (Larocca et al., 2004). We found that the expression of CIP4BD decreased the fraction of cells in which the centrosomes and Golgi had polarized (Fig. 6D).

Journal of Cell Science (2015) 128, 3277-3289 doi:10.1242/jcs.170878

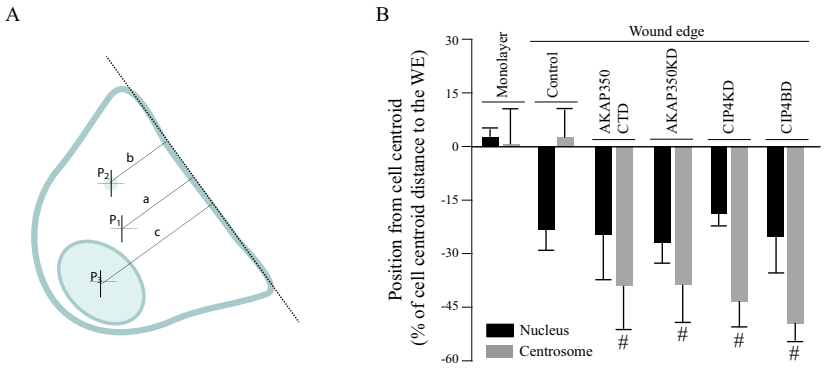

Fig. 7. Positioning of the centrosome and the nucleus in cells with decreased AKAP350 or CIP4 function. (A) Schematic showing the methodology used to determine the position of the nucleus and the centrosome in cells at the wound edge. The wound direction was determined by outlining a line tangent to the wound edge (dashed line) by using DIC images. The cell perimeter was drawn, and the cell centroid (p1) coordinates estimated using ImageJ tools. Similarly, the centrosome and the nucleus areas were automatically determined using binary images of γ-tubulin and DAPI staining in order to determine the centrosomal (p2) and nuclear (p3) centroid coordinates. The difference between the distance from the centroid of the centrosome (b) or the nucleus (c) and the distance from the cell centroid (a) to the line tangent to the leading edge was calculated, and divided by the distance from the cell centroid to the leading edge (a). Negative values refer to organelle localization behind the cell centroid, whereas positive values indicate organelle localization in front of the nucleus. (B) Bar graph illustrates the position of the centrosome (gray) or the nucleus (black) in cells at the wound edge (WE) and cells located four lines behind the wound edge (monolayer). Data are expressed as means±s.e.m. of at least 40 cells, representative of three independent experiments. $^{\#}P<0.05$ compared to control organelles.

AKAP350 and CIP4 determine centrosome position but not nuclear movement

Depending on the cell type, the relocation of the centrosome relative to the nucleus, which is required for migratory front–rear polarity, might be secondary to centrosome movement to the leading edge (Etienne-Manneville and Hall, 2001) or to nuclear relocation to the back of the cell, with active retention of the centrosome at its central position (Gomes et al., 2005). Therefore, we evaluated whether the interference with AKAP350 and CIP4 functions inhibited centrosome localization in front of the nucleus by impeding nuclear or centrosome location. We measured the distances from the centroid of the nucleus and from the centrosome to the leading edge, and compared them with the distance from the centroid of the cell to the leading edge, both in cells at the wound edge and in cells in the monolayer (Fig. 7A). The nucleus and centrosome of cells in the monolayer were located at the cell center (nucleus, 0.2 µm± 0.2 µm; centrosome, 0.1 µm±1.0 µm), and these locations were unaffected by changes in AKAP350 or CIP4 expression (data not shown). Similar to that which occurs in fibroblasts, the nucleus moved rearward (−2.2 µm±0.6 µm), whereas the centrosome remained at the cell center (0.3 µm±0.7 µm) in HepG2 control cells at the edge of the wound. The position of the nucleus relative to the cell centroid was unaltered in AKAP350CTD, AKAP350KD, CIP4KD or CIP4BD cells, indicating that movement of the nucleus was unaffected by AKAP350 or CIP4 loss of function. By contrast, the decrease in AKAP350 expression or its delocalization from the centrosome, as well as the decrease in CIP4 expression or the inhibition of its interaction with AKAP350, led to localization of the centrosome behind the cell centroid (Fig. 7B). Similarly, loss of AKAP350 function led to relocation of the centrosome to the back of the cell in MDCK migrating cells (centrosome, 1.3 µm±0.6 µm; AKAP350KD, −1.1 µm±0.7 µm*; AKAP350CTD, −2.9 µm± 1.0 µm*; *$P<0.01$), without affecting the position of the nucleus at the back of the cell. These results indicate that, during the acquisition of a migratory phenotype, the nucleus moved away from the wound edge, whereas the centrosome remained at the cell center in HepG2 cells or moved slightly forward in MDCK cells. Perturbing the AKAP350–CIP4 pathway led to relocalization of the centrosome to the back of the cell in both cell types.

The actin cytoskeleton is involved in positioning the centrosome and nucleus in migrating cells

There is experimental data supporting the presence of an actin-mediated interaction between the nucleus and the centrosome (Burakov and Nadezhdina, 2013); therefore, we analyzed the effect of actin depolymerization at the moment of scratch wounding on the position of the centrosome with respect to the cell center and to the nucleus in AKAP350CTD, AKAP350KD and CIP4KD cells. We found that pre-treatment with cytochalasin D could restore positioning of the centrosome in front of the nucleus in every case (Fig. 8), thus supporting the notion that actin prevents dissociation of the centrosome from the movement of the nucleus during the acquisition of the migratory polarity in these cells. Interestingly, cytochalasin-D-pre-treated AKAP350CTD cells migrated as efficiently as control cells (data not shown), thus confirming that the alteration in centrosome polarity is the leading cause of the impaired cell migration in these cells.

DISCUSSION

Directional cell movement is a complex phenomenon, which requires the concerted, networked action of an extensive collection of structural and regulatory proteins. In this scenario, the elucidation of how regulatory signals are integrated with structural responses appears to be crucial. In the last decades, many studies have focused on the early polarity signals that define the establishment of the front–rear polarity, which is essential in the acquisition of the migratory phenotype. An important, but still not completely understood, question is how the spatial cues lead to the centrosome reorientation in the direction of migration. In this context, the involvement of cdc42 activation at the front of the cell as a symmetry-breaking signal has been well characterized (Nelson, 2009). Cdc42 activation at the anterior pole leads to movement of the nucleus towards the back of the cell, and to relocalization of the centrosome and Golgi complex between the nucleus and the leading edge in diverse cell models (Palazzo et al., 2001; Etienne Maneville and Hall, 2001; Tzima et al., 2003). Regarding centrosome positioning, these studies point to a cdc42–Par6-dependent dynein activation at the leading edge, leading to microtubule pulling of the centrosome and the subsequent positioning of the centrosome in

Journal of Cell Science (2015) 128, 3277-3289 doi:10.1242/jcs.170878

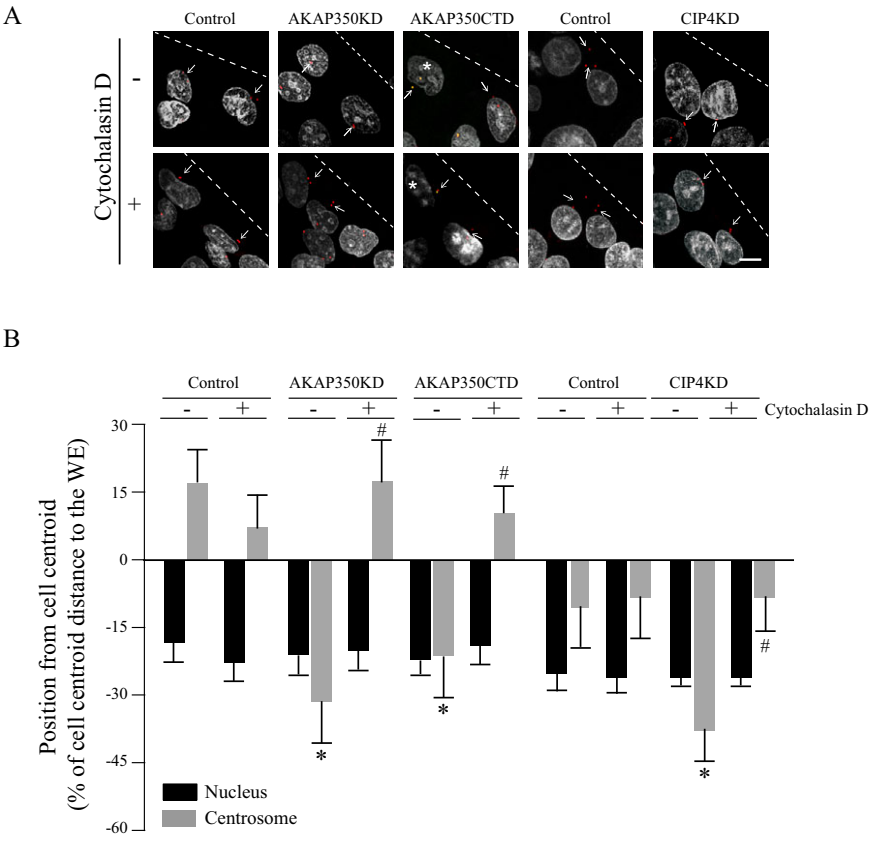

Fig. 8. Effect of actin depolymerization at the moment of scratch wounding on centrosome and nuclear positioning. Cells were treated with cytochalasin D 30 min before scratch wounding and kept in cytochalasin-D-containing medium for the subsequent 20 min. Afterwards, cells were allowed to migrate in the absence of the toxin for 3 h (MDCK) or 6 h (HepG2). Cells were stained and analyzed by using quantitative confocal microscopy, as described in Fig. 7, to determine nucleus and centrosome positioning relative to the cell center. (A) Merged images show γ-tubulin (red) and DAPI (gray) staining. Asterisks indicate AKAP350CTD cells, where centrosomes show γ-tubulin (red) and AKP350CTD (green) colocalization, and arrows indicate the position of the centrosomes corresponding to cells at the wound edge (WE; dashed lines). (B) Bar graph shows the position of the centrosome (gray) or the nucleus (black) in AKAP350CTD and AKAP350KD MDCK cells, and CIP4KD HepG2 cells at the wound edge in the presence (+) or absence (–) of pre-treatment with cytochalasin D. Data are expressed as means±s.e.m. of at least 40 cells representative of three independent experiments. **P*<0.05 compared to control centrosomes, $^{\#}P$<0.05 compared to the position of the organelle in the absence of cytochalasin D. Scale bar: 10 µm.

front of the nucleus (Palazzo et al., 2001; Etienne Maneville and Hall, 2001; Dujardin et al., 2003). In the present study, we aimed to characterize the centrosomal players of the polarized positioning of this organelle and its functional partner, the Golgi complex, which have not been identified so far. We focused on two proteins that are involved in cell migration – the centrosome and Golgi scaffold protein AKAP350 and the cdc42 effector CIP4.

AKAP350 has been identified as a crucial participant in cell migration in different cell contexts, including integrin-induced T-cell migration, and epithelial and melanoma cell migration in experimental wounding (El Din El Homasany et al., 2005; Rivero et al., 2009; Kabbarah et al., 2010). Previous studies suggest that AKAP350 facilitates directional cell migration by enabling microtubule nucleation at the Golgi (Rivero et al., 2009), which is necessary for proper trafficking of membrane components towards the leading edge (Efimov et al., 2007). Nevertheless, this mechanism does not explain the defective cell migration that is induced through displacement of AKAP350 from the centrosomes in T cells. Considering that centrosome behavior varies widely between different types of cell (Tang and Marshall, 2012), we first analyzed the effect of AKAP350 displacement from the centrosomes on cell migration in different cell types. We found that centrosomal AKAP350 participates in cell migration in non-immune cells, including those derived from hepatocellular carcinoma (HepG2, hepatocytes) and liver adenocarcinoma (SK-Hep1, endothelial cells), as well as in immortalized epithelial MDCK cells. Regarding reorientation of the Golgi and centrosomes, Rivero et al. (2009) report that this is unaffected by a decrease in AKAP350 expression in RPE1 cells. We found that both the displacement of centrosomal AKAP350 and the decrease in the total expression of the protein led to inhibition of centrosome and Golgi polarization within HepG2 cells. In order to determine whether these observations were a peculiarity of the cell type used, we further analyzed this phenomenon in SK-Hep1 and MDCK cells, and confirmed that centrosomal AKAP350 is essential in this process. Thus, the results of previous studies could be either a peculiarity of RPE1 cells, or related to efficiency of the knockdown of AKAP350. Centrosomal microtubules play a central role in the organization of the Golgi complex (Vinogradova et al., 2012). AKAP350 itself participates in the maintenance of the Golgi architecture (Larocca et al., 2004), which conditions centrosomal positioning in migratory cells (Sutterlin and Colanzi, 2010). Furthermore, Hurtado and colleagues (2011) show that overexpression of the N-terminal Golgi-targeting domain of AKAP350 inhibits both centrosome and Golgi reorientation towards the leading edge. We investigated whether the impairment in centrosomal repositioning that was induced by AKAP350 delocalization from the centrosomes was secondary to the direct effects on the Golgi. We found that neither AKAP350 levels at the Golgi nor Golgi stacking were modified in non-migratory AKAP350CTD cells. In addition, the Golgi levels of GM130, an AKAP350 partner at the Golgi that participates in centrosome positioning during the acquisition of migratory polarity (Kodani and Sütterlin, 2008), are preserved in AKAP350CTD cells. Hence, these studies provide strong evidence for the direct involvement of centrosomal AKAP350 in centrosome and Golgi positioning in front of the nucleus in migratory cells. Interestingly, centrosomal AKAP350 participates in centrosome reorientation towards the site of interaction with target cells (immunological synapsis) during Jurkat T-cell activation (Robles-Valero et al., 2010). Similar to the development of the front–rear polarity in migratory cells, an early event in the development of the immunological synapsis is the polarized activation of cdc42 at the interface between the immune cell and the target cell. Therefore,

Journal of Cell Science (2015) 128, 3277-3289 doi:10.1242/jcs.170878

AKAP350 is involved in different types of centrosomal movement that are induced by cues which originate at the plasma membrane, implicating cdc42 activation.

CIP4 is a scaffold protein, which acts downstream of cdc42 to modulate membrane curvature in several processes, such as endocytosis and the formation of membrane protrusions. In contrast to the identification of CIP4 as a membrane-associated protein, Banerjee et al. (2007) have demonstrated that, upon interaction of natural killer cells with target cells, CIP4 colocalizes with centrosomal markers. The centrosomal localization of CIP4 in non-immune cells and the mechanism that mediates localization of CIP4 at the only non-membranous organelle had not been investigated so far. In the present study, by using two different approaches, we found that CIP4 localizes at the centrosomes in HepG2 cells. Regarding the mechanism, CIP4 interacts with AKAP350 by means of an amino acid sequence located in the F-BAR domain (Larocca et al., 2004). We further showed that cells expressing the AKAP350 centrosomal targeting domain (AKAP350CTD) have, on average, a 50% decrease in centrosomal CIP4, which is very similar to the fraction of AKAP350 that delocalizes from the centrosomes in these cells. Therefore, our results provide crucial evidence that supports the concept that AKAP350 is responsible for CIP4 recruitment to the centrosomes. It will be interesting to investigate whether this interaction is also responsible for CIP4 recruitment to the centrosome in different models of cell polarity.

Similar to AKAP350, CIP4 has been implicated in cell migration in several cell contexts. CIP4 is overexpressed in normal epithelial cells undergoing the epithelial–mesenchymal transition (Zhang et al., 2013). CIP4 is also overexpressed in osteosarcoma (Koshkina et al., 2013), in chronic lymphocytic leukemia (Malet-Engra et al., 2013), in non-small cell lung cancer (Truesdell et al., 2014) and in a subset of invasive breast cancer cells (Pichot et al., 2010). In every case, interfering with CIP4 function leads to defective cell migration. CIP4 also participates in integrin-induced T-cell migration (Bai et al., 2012). The mechanisms by which CIP4 conditions cell migration remain unclear. F-BAR proteins participate in the development of lamellipodia, structures that are highly relevant for cell migration. In fact, CIP4 promotes lamellipodia formation in cortical neurons (Saengsawang et al., 2012) and localizes at the leading edge in tumor cells (Pichot et al., 2010; Truesdell et al., 2014). A recent study has shown that CIP4 regulates cell cohesion by modulating E-cadherin endocytosis and the actomyosin contraction required to break cell–cell junctions, thus facilitating cell migration (Rolland et al., 2014). Therefore, previous studies support the hypothesis that CIP4 participates in cell migration through its canonical role in integrating membrane deformation and actin dynamics. We found that the specific decrease of CIP4 protein levels leads to a marked inhibition in the polarization of the centrosome and Golgi within the cell. Furthermore, we showed that not only CIP4 expression but also its proper interaction with AKAP350 is necessary for centrosome and Golgi positioning in migrating cells, thus ruling out that this phenomenon is secondary to CIP4 regulation of membrane plasticity. Hence, our results strongly suggest that cells express a centrosomal pool of CIP4 that participates in cell migration by modulating centrosome and Golgi reorientation during the acquisition of front–rear polarity. Likewise, during the interaction of natural killer cells with their targets, CIP4 acts downstream of cdc42 to enable translocation of the centrosome towards the immune synapse (Banerjee et al., 2007). CIP4 participation in other processes that require centrosome positioning, such as cilia formation, represents an appealing subject for future studies.

Movement of the nucleus towards the back of the cell is a common feature of most migrating cells. In fibroblasts, it has been established that nuclear positioning is driven by actin retrograde flow, which requires myosin II phosphorylation that is downstream of cdc42 activation (Gomes et al., 2005). In the present study, we found that neither AKAP350 nor CIP4 are necessary for relocation of the nucleus to the back of the cell, thus indicating that movement of the nucleus is unaffected and that the early stages of establishing migratory polarity are conserved in these cells. Our results also indicate that loss of function of both CIP4 and AKAP350 not only leads to a lack of centrosome localization in front of the nucleus but also to localization of the centrosome behind the nucleus, thus suggesting nuclear dragging of this organelle towards the back of the cell. We further investigated which mechanisms could condition these phenomena. The functional connection between the nucleus and the centrosome is supported by several *in vivo* observations, but the actual existence of a physical link has never been confirmed in mammalian epithelia-like cells. Furthermore, the nature of this interaction is controversial. Although most of the evidence on this matter points to the microtubule cytoskeleton as a connector between these organelles, there is methodological *in vitro* evidence suggesting that actin or actin-associated fibers are involved in nucleus–centrosome binding (Burakov and Nadezhdina, 2013). Previous studies demonstrate the presence of actin regulatory proteins at the centrosome (Hubert et al., 2010). Thus, we hypothesized that, during the acquisition of migratory polarity, AKAP350 recruits CIP4 to the centrosome, positioning it close to signaling proteins that could regulate actin dynamics at the centrosome and, thus, promote the centrosome disengagement from the nucleus. Our results showed that conditions that led to actin depolymerization at the moment of scratch wounding, re-establish the normal centrosomal polarized phenotype in AKAP350CTD, AKAP350KD and CIP4KD cells. To our knowledge, this is the first functional evidence to support the idea that the actin cytoskeleton participates in the nucleus–centrosome interaction, and this is in line with our hypothesis that the presence of CIP4 at the centrosome is necessary to disengage the centrosome from the nucleus by allowing actin remodeling. In this regard, CIP4 interacts with DAAM1, which is a formin protein belonging to the diaphanous family (Aspenström et al., 2006). Interestingly, DAAM1 localizes to the acto-myosin fibers in the centrosomal area and participates in centrosome reorientation during the acquisition of migratory polarity (Ang et al., 2010). Thus, it would be interesting to investigate if, by binding to this formin, CIP4 can regulate the association of centrosomes with actin fibers and, thus, centrosome positioning in migrating cells. Therefore, during the acquisition of the migratory polarity, AKAP350 can define centrosome positioning relative to the nucleus and to the cell center by integrating microtubule and actin dynamics (Tang and Marshall, 2012) – thus AKAP350 provides a site for microtubule anchorage and, by providing a site for the localization of CIP4 at this organelle, it could also regulate actin dynamics.

Overall, the present study establishes that the scaffold protein AKAP350 and the cdc42 effector CIP4 participate in centrosomal events that are central to the acquisition of the migratory phenotype, and provide evidence of a direct connection between the two proteins in this function. There is growing evidence supporting the relevance of the events characterized here for a diverse range of processes, such as immune synapse formation, integrin-induced T-cell migration and tumor cell metastasis.

Journal of Cell Science (2015) 128, 3277-3289 doi:10.1242/jcs.170878

MATERIALS AND METHODS

Cell culture and treatments

HepG2, Sk-Hep1 and MDCK cells (obtained from American Type Culture Collection) were grown on plastic dishes in Dulbecco's modified Eagle's medium (DMEM) with 4.5 g of glucose/l, supplemented with 10% fetal bovine serum and antibiotics.

Reduction of CIP4 and AKAP350 expression by RNA interference

In order to reduce protein expression in HepG2 cells, specific 21-nucleotide double-chain RNA [small interfering (si)RNA] and a scrambled control were designed, as we have previously described (Mattaloni et al., 2012), and synthesized using an Ambion commercial kit 'SilencerTMsiRNA'. The following sequences targeting *AKAP350* or *CIP4* mRNA were used – AKAP350 siRNA1 5′-AAATCCCTTGCCAGCACATGA-3′, AKAP350 siRNA2 5′-AAGCAAGAACTAGAACGAGAA-3′ and CIP4 siRNA 5′-GACCTCAGTCTTATGGAAGAA-3′. Cells were transfected using Dharmafect 4 reagent (Thermo Fisher Scientific). Experiments were performed 48 h after transfection, and the specific decrease in AKAP350 or CIP4 expression was confirmed by immunoblotting and immunofluorescence analyses.

In order to reduce AKAP350 expression in MDCK cells, we proceeded as we have described previously (Lepanto et al., 2011). Constructs were made by annealing and ligating oligonucleotides targeting *AKAP350* sequences (shRNA1, 5′-CCCAGCTCACTGCTAATTT-3′; shRNA4, 5′-GCAAGAACTAGAACGAGAA-3′) into the *Age*I and *Eco*RI cloning sites of pLKO.1-puro vector (details at http://www.addgene.org). These constructs were sequenced and used to co-transfect human embryonic kidney 293 FT cells with Virapower lentiviral packaging mix (Invitrogen, Carlsbad, CA). The next day, transfection complexes were removed, and cells were allowed to produce virus for 24 h. Media containing virus were collected and used to directly transduce MDCK cells overnight. The cells were allowed to recover for 24 h and subjected to puromycin selection (5 µg/ml) for 2 weeks. Silencing was confirmed by western blotting and immunofluorescence analyses.

Generation of stable cell lines (AKAP350CTD)

The AKAP350(3330–3595) domain, equivalent to AKAP450(3643–3908), was cloned into pEGFP-C2 (Clontech) to generate a construct coding for GFP fused to the C-terminal domain of AKAP350 (AKAP350CTD–GFP). Populations of cells that stably expressed AKAP350CTD–GFP or GFP (control) were generated. HepG2 cells were transfected by using electroporation, as previously described (Mattaloni et al., 2012). Sk-Hep1 and MDCK cells were transfected using Amaxa Nucleofector™ 2b with program X-001. After 24 h, the antibiotic Geneticin (Invitrogen, 500 µg/ml) was added to the medium in order to select the transfected cells. These cell lines were maintained in a medium containing Geneticin 200 µg/ml in conditions that were otherwise similar to those used to maintain parental cells.

GFP–AKAP350(1076–2143) and CIP4–GFP expression

The AKAP350(1076–2143) domain was cloned into pEGFP-C2, as previously described (Larocca et al., 2004). Full-length *CIP4* cDNA that had been cloned into pRK5, as described previously (Tian et al., 2000), was used as a template to clone *CIP4* into the pEGFP-N1 vector (Clontech) by using *Eco*R1 and *Sal*I sites, generating a construct coding for CIP4 fused to the N-terminus of GFP. HepG2 cells were transfected with these constructs using FuGENE (ProMega).

Wound healing assay

Cells seeded at 2.5×10^6 in 2 ml of DMEM were cultured overnight at 37°C in 6-well plates. After 24 h, cells were wounded by dragging a 100-µl pipette tip through the monolayer. Cells were washed using PBS to remove cellular debris and allowed to migrate. In order to analyse the involvement of the actin cytoskeleton in centrosomal reorientation, cells were treated with cytochalasin D (4 µM) 30 min before scratch wounding and then maintained in a lower dose (0.25 µM) for 20 min. Afterwards, cells were washed three times with PBS and allowed to migrate in the absence of the toxin. In one set of experiments, images of wounds in the same field were captured when the scrape wound was introduced (0 h) and at designated periods after wounding (24 and 40 h) using an inverted microscope. The relative wound closure was assessed by using ImageJ software (Kong et al., 2011). Alternatively, cells were fixed at different periods after the wound was performed and analysed by using immunofluorescence confocal microscopy.

Immunoblotting

AKAP350 and CIP4 protein expression was analyzed as previously described (Larocca et al., 2004). Briefly, cells were washed with cold PBS, scraped and pelleted at 200 ***g*** for 5 min at 4°C. Pelleted cells were resuspended in Triton X-100 1% in PBS pH 7.4 with protease and phosphatase inhibitors, and subjected to two freeze–thaw cycles. Lysates were centrifuged at 1000 ***g*** for 5 min, and the clear supernatants were conserved. Total protein concentrations were measured according to Lowry et al. (1951) Solubilized membranes were heated for 10 min at 70°C in sample buffer (20 mM Tris-HCl, pH 8.5, 1% SDS, 400 µM DTT, 10% glycerol). Samples containing equal amounts of protein were subjected to SDS 4% or 12% polyacrylamide gel electrophoresis. The proteins in the gel were transferred to polyvinyl difluoride membranes. Blots were blocked with 5% non-fat milk in PBS with 0.3% Tween-20. Membranes were probed with mouse monoclonal antibodies against AKAP350 (Schmidt et al., 1999), CIP4 (1:500, BD Biosciences), γ-tubulin (1:5000, Sigma) and α-tubulin (1:5000, Sigma). The blots were washed and incubated with the corresponding horseradish-peroxidase-conjugated secondary antibodies. Bands were detected by using chemiluminescence reaction (Pierce, Thermo Scientific) after exposure to Kodak XAR film. Bands were quantified using the ImageJ program. In preparing the figures, brightness and contrast were adjusted in order to improve visualization.

Immunofluorescence confocal microscopy

The cells were grown on glass coverslips and, at the end of each experiment, washed with PBS and fixed with 4% paraformaldehyde at room temperature or in 100% methanol at −20°C. Fixed cells were permeabilized and blocked with 0.3% Triton X-100 with 1% bovine serum albumin in PBS, pH 7.4, for 10 min. Then, they were incubated with monoclonal rabbit antibodies against GM130 (Abcam, 1:300) or γ-tubulin (1:250) or monoclonal mouse antibodies against γ-tubulin (1:500), AKAP350 (1:80) or CIP4 (1:80) for 2 h. The coverslips were washed, incubated for 1 h with the secondary fluorescence-conjugated antibodies and with 4′,6-diamidino-2-phenylindole (DAPI) and mounted with ProLong. Fluorescence was detected by using confocal laser microscopy (Nikon C1SiR with inverted microscope Nikon TE200). Serial optical 0.3-µm thick sections were collected in the *z*-axis. *z*-stacks were built, and projections were obtained using ImageJ tools. In preparing the figures, adjustment in brightness and contrast were equally applied to the entire images using Adobe Photoshop software, in order to improve visualization of fluorescence.

Analysis of centrosome and Golgi polarity

The Golgi was stained using an antibody against GM130, and the centrosomes were stained with anti-γ-tubulin antibodies. Golgi and centrosome orientation were determined for the first row of cells facing the wound, as described previously (Etienne-Manneville and Hall, 2001; Gomes et al., 2005), and counted as oriented if the majority was located in a 120° sector emerging from the center of the nucleus and facing the wound edge. The percentage of cells with Golgi or centrosome polarization was calculated by dividing the number of cells with the organelle oriented towards the leading edge by the number of total cells for each condition.

Determination of nucleus and centrosome position

Differential interference contrast (DIC) and fluorescence images of cells stained for γ-tubulin, GM130 and DAPI were acquired as previously described (Palazzo et al., 2001). The position of the nucleus and the centrosome relative to the cell centroid in the cells located at the wound edge, and in cells located four lines behind the wound, was determined in a manner similar to that previously described (Gomes et al., 2005). A line tangent to the wound edge was outlined using DIC images, and its slope and

one (x,y) coordinate measured. The cell perimeter was drawn over the cell–cell contacts, and the cell centroid x,y coordinates estimated. Similarly, the nuclear and the centrosomes perimeter were delimited by using an automatic selection tool, and the centroid of both organelles was located. The distance from the cell centroid to the line tangent to the leading edge, and the difference between the distance from the centroid of the nucleus or the centrosome and the distance from the cell centroid to the line tangent to the leading edge were calculated. All the measurements were performed using the appropriate ImageJ tools. At least 30 cells from three independent experiments were analyzed for each condition.

Analysis of protein localization

Protein localization at centrosomes and Golgi in control and AKAP350CTD cells was assessed in images obtained from mixed populations of cells, so that the same image acquisition settings, background corrections and thresholds were applied for both groups of cells.

Centrosomes

Centrosomal localization of CIP4 was determined in images obtained by using confocal microscopy by setting a threshold on the γ-tubulin channel to define a mask, which was used to automatically outline the centrosomal voxels, and a threshold on the CIP4 channel to define a mask to automatically outline total voxels for CIP4 staining. The average intensity of fluorescence in the CIP4 channel was measured in each region of interest, and the ratio of centrosomal to total cell average levels calculated. Alternatively, we prepared centrosome-enriched fractions by centrifuging in a sucrose gradient, using a method based on that of Moudju and Bornens (1994), modified to improve resolution of centrosomal proteins (Moritz et al., 1995). Cells were gently sonicated in cold buffer containing 80 mM HEPES (pH 6.8), 100 mM KCl, 14% sucrose, 1 mM $MgCl_2$, 1 mM EGTA and protease inhibitors. In order to eliminate unbroken cells and nuclear fractions, cell extracts were centrifuged at 1500 ***g*** for 15 min. The sucrose content of the supernatant was increased to 20% sucrose, 0.1% Triton X-100, and loaded onto the top of a sucrose step-gradient comprising 70% and 40% steps. Samples were centrifuged at 100,000 ***g*** for 20 min, and six fractions corresponding to the 40–70% sucrose fractions were collected. The best enrichment of centrosomes, assessed by γ-tubulin distribution, was obtained at the fraction corresponding to the 40–70% interface.

Golgi complex

Golgi levels of AKAP350 and GM130 were determined in images obtained by using confocal microscopy by setting a threshold on the GM130 channel to define a mask, which was used to automatically outline the Golgi voxels. Total intensity of fluorescence in the GM130 and AKAP350 channels were measured in each region of interest. In addition, the total AKAP350 levels were determined in a region delimited by a mask defined using the AKAP350 channel, and the percentage of AKAP350 fluorescence at the Golgi was calculated.

Statistical analysis

Data are expressed as mean±s.e.m. and are representative of at least three experiments. Paired Student's *t*-test was used for comparison between experiments, or for comparisons within each experiment when mixed populations of cells were used. Otherwise, non-parametric Mann–Whitney test was used for comparisons within each experiment. $P<0.05$ was considered statistically significant.

Acknowledgements

We thank R. Vena and Dr P. Cribb (Instituto de Biología Molecular y Celular de Rosario – CONICET, Argentina), and J. Marrone (Instituto de Fisiología Experimental - CONICET, Argentina) for their technical assistance; and Dr E. Serra (Facultad de Ciencias Bioquímicas y Farmacéuticas - UNR, Argentina) for providing reagents crucial for this work.

Competing interests

The authors declare no competing or financial interests.

Author contributions

F.M.T., A.K. and M.C.L. designed the study. F.M.T., F.H., A.C.F., E.A. and M.C.L. performed the experiments and analysed the data. F.M.T., C.F., J.R.G., I.K. , A.K., and M.C.L. discussed the data and wrote the manuscript.

Funding

This work was supported by Consejo Nacional de Investigaciones Científicas y Técnicas [grant number PIP0287 to M.C.L.]; Agencia Nacional de Promoción Científica y Tecnológica [grant numbers PICT 2012-2198 (to M.C.L.) and PICT 2013-3291 (to A.K.)]; Argentina Government (BEC.AR fellowship to F.M.T.); and by the National Institutes of Health [grant number RO1 DK43405 to J.R.G.]. Deposited in PMC for release after 12 months.

References

Ang, S.-F., Zhao, Z.-S., Lim, L. and Manser, E. (2010). DAAM1 is a formin required for centrosome re-orientation during cell migration. *PLoS ONE* **5**, e13064.

Aspenström, P. (1997). A Cdc42 target protein with homology to the non-kinase domain of FER has a potential role in regulating the actin cytoskeleton. *Curr. Biol.* **7**, 479-487.

Aspenström, P., Richnau, N. and Johansson, A. S. (2006). The diaphanous-related formin DAAM1 collaborates with the Rho GTPases RhoA and Cdc42, CIP4 and Src in regulating cell morphogenesis and actin dynamics. *Exp. Cell Res.* **312**, 2180-2194.

Bai, S., Zeng, R., Zhou, Q., Liao, W., Zhang, Y., Xu, C., Han, M., Pei, G., Liu, L., Liu, X. et al. (2012). Cdc42-interacting protein-4 promotes TGF-B1-induced epithelial-mesenchymal transition and extracellular matrix deposition in renal proximal tubular epithelial cells. *Int. J. Biol. Sci.* **8**, 859-869.

Banerjee, P. P., Pandey, R., Zheng, R., Suhoski, M. M., Monaco-Shawver, L. and Orange, J. S. (2007). Cdc42-interacting protein-4 functionally links actin and microtubule networks at the cytolytic NK cell immunological synapse. *J. Exp. Med.* **204**, 2305-2320.

Burakov, A. V. and Nadezhdina, E. S. (2013). Association of nucleus and centrosome: magnet or velcro? *Cell Biol. Int.* **37**, 95-104.

Dujardin, D. L., Barnhart, L. E., Stehman, S. A., Gomes, E. R., Gundersen, G. G. and Vallee, R. B. (2003). A role for cytoplasmic dynein and LIS1 in directed cell movement. *J. Cell Biol.* **163**, 1205-1211.

Efimov, A., Kharitonov, A., Efimova, N., Loncarek, J., Miller, P. M., Andreyeva, N., Gleeson, P., Galjart, N., Maia, A. R. R., McLeod, I. X. et al. (2007). Asymmetric CLASP-dependent nucleation of noncentrosomal microtubules at the trans-Golgi network. *Dev. Cell* **12**, 917-930.

El Din El Homasany, B. S., Volkov, Y., Takahashi, M., Ono, Y., Keryer, G., Delouvée, A., Looby, E., Long, A. and Kelleher, D. (2005). The scaffolding protein CG-NAP/AKAP450 is a critical integrating component of the LFA-1-induced signaling complex in migratory T cells. *J. Immunol.* **175**, 7811-7818.

Etienne-Manneville, S. (2013). Microtubules in cell migration. *Annu. Rev. Cell Dev. Biol.* **29**, 471-499.

Etienne-Manneville, S. and Hall, A. (2001). Integrin-mediated activation of Cdc42 controls cell polarity in migrating astrocytes through PKCzeta. *Cell.* **106**, 489-498.

Feng, Y., Hartig, S. M., Bechill, J. E., Blanchard, E. G., Caudell, E. and Corey, S. J. (2010). The Cdc42-interacting protein-4 (CIP4) gene knock-out mouse reveals delayed and decreased endocytosis. *J. Biol. Chem.* **285**, 4348-4354.

Fricke, R., Gohl, C., Dharmalingam, E., Grevelhörster, A., Zahedi, B., Harden, N., Kessels, M., Qualmann, B. and Bogdan, S. (2009). Drosophila Cip4/Toca-1 integrates membrane trafficking and actin dynamics through WASP and SCAR/WAVE. *Curr. Biol.* **19**, 1429-1437.

Gillingham, A. K. and Munro, S. (2000). The PACT domain, a conserved centrosomal targeting motif in the coiled-coil proteins AKAP450 and pericentrin. *EMBO Rep.* **1**, 524-529.

Gomes, E. R., Jani, S. and Gundersen, G. G. (2005). Nuclear movement regulated by Cdc42, MRCK, myosin, and actin flow establishes MTOC polarization in migrating cells. *Cell* **121**, 451-463.

Hartig, S. M., Ishikura, S., Hicklen, R. S., Feng, Y., Blanchard, E. G., Voelker, K. A., Pichot, C. S., Grange, R. W., Raphael, R. M., Klip, A. et al. (2009). The F-BAR protein CIP4 promotes GLUT4 endocytosis through bidirectional interactions with N-WASp and Dynamin-2. *J. Cell Sci.* **122**, 2283-2291.

Hu, J., Mukhopadhyay, A., Truesdell, P., Chander, H., Mukhopadhyay, U. K., Mak, A. S. and Craig, A. W. B. (2011). Cdc42-interacting protein 4 is a Src substrate that regulates invadopodia and invasiveness of breast tumors by promoting MT1-MMP endocytosis. *J. Cell Sci.* **124**, 1739-1751.

Hubert, T., Vandekerckhove, J. and Gettemans, J. (2011). Actin and Arp2/3 localize at the centrosome of interphase cells. *Biochem. Biophys. Res. Commun.* **404**, 153-158.

Hurtado, L., Caballero, C., Gavilan, M. P., Cardenas, J., Bornens, M. and Rios, R. M. (2011). Disconnecting the Golgi ribbon from the centrosome prevents directional cell migration and ciliogenesis. *J. Cell Biol.* **193**, 917-933.

Kabbarah, O., Nogueira, C., Feng, B., Nazarian, R. M., Bosenberg, M., Wu, M., Scott, K. L., Kwong, L. N., Xiao, Y., Cordon-Cardo, C. et al. (2010). Integrative

genome comparison of primary and metastatic melanomas. *PLoS ONE* **5**, e10770.
Kodani, A. and Sütterlin, C. (2008). The Golgi protein GM130 regulates centrosome morphology and function. *Mol. Biol. Cell* **19**, 745-753.
Kong, G., Zhang, J., Zhang, S., Shan, C., Ye, L. and Zhang, X. (2011) Upregulated microRNA-29a by hepatitis B virus X protein enhances hepatoma cell migration by targeting PTEN in cell culture model. *PLoS One.* **6**, e19518.
Koshkina, N. V., Yang, G. and Kleinerman, E. S. (2013). Inhibition of Cdc42-interacting protein 4 (CIP4) impairs osteosarcoma tumor progression. *Curr. Cancer Drug Targets* **13**, 48-56.
Larocca, M. C., Shanks, R. A., Tian, L., Nelson, D. L., Stewart, D. M. and Goldenring, J. R. (2004). AKAP350 interaction with cdc42 interacting protein 4 at the Golgi apparatus. *Mol. Biol. Cell* **15**, 2771-2781.
Larocca, M. C., Jin, M. and Goldenring, J. R. (2006). AKAP350 modulates microtubule dynamics. *Eur. J. Cell Biol.* **85**, 611-619.
Leibfried, A., Fricke, R., Morgan, M. J., Bogdan, S. and Bellaiche, Y. (2008). Drosophila Cip4 and WASp define a branch of the Cdc42-Par6-aPKC pathway regulating E-cadherin endocytosis. *Curr. Biol.* **18**, 1639-1648.
Lepanto, P., Bryant, D. M., Rossello, J., Datta, A., Mostov, K. E. and Kierbel, A. (2011). Pseudomonas aeruginosa interacts with epithelial cells rapidly forming aggregates that are internalized by a Lyn-dependent mechanism. *Cell. Microbiol.* **13**, 1212-1222.
Lowry, O. H., Rosebrough, N. J., Farr, A. L. and Randall, R. J. (1951). Protein measurement with the Folin phenol reagent. *J. Biol. Chem.* **193**, 265-275.
Malet-Engra, G., Viaud, J., Ysebaert, L., Farcé, M., Lafouresse, F., Laurent, G., Gaits-Iacovoni, F., Scita, G. and Dupré, L. (2013). CIP4 controls CCL19-driven cell steering and chemotaxis in chronic lymphocytic leukemia. *Cancer Res.* **73**, 3412-3424.
Mattaloni, S. M., Kolobova, E., Favre, C., Marinelli, R. A., Goldenring, J. R. and Larocca, M. C. (2012). AKAP350 is involved in the development of apical "canalicular" structures in hepatic cells HepG2. *J. Cell. Physiol.* **227**, 160-171.
Mattaloni, S. M., Ferretti, A. C., Tonucci, F. M., Favre, C., Goldenring, J. R. and Larocca, M. C. (2013). Centrosomal AKAP350 modulates the G1/S transition. *Cell. Logist.* **3**, e26331.
Moritz, M., Braunfeld, M. B., Fung, J. C., Sedat, J. W., Alberts, B. M. and Agard, D. A. (1995). Three-dimensional structural characterization of centrosomes from early Drosophila embryos. *J. Cell. Biol.* **130**, 1149-1159.
Moudjou, M. and Bornens, M. (1994) Isolation of centrosomes from cultured animal cells, in Cell Biology: A Laboratory Handbook. (ed. J. E. Celis), pp. 595–604. San Diego:Academic Press.
Nelson, W. J. (2009). Remodeling epithelial cell organization: transitions between front-rear and apical-basal polarity. *Cold Spring Harb. Perspect. Biol.* **1**, a000513.
Palazzo, A. F., Joseph, H. L., Chen, Y.-J., Dujardin, D. L., Alberts, A. S., Pfister, K. K., Vallee, R. B. and Gundersen, G. G. (2001). Cdc42, dynein, and dynactin regulate MTOC reorientation independent of Rho-regulated microtubule stabilization. *Curr. Biol.* **11**, 1536-1541.
Pichot, C. S., Arvanitis, C., Hartig, S. M., Jensen, S. A., Bechill, J., Marzouk, S., Yu, J., Frost, J. A. and Corey, S. J. (2010). Cdc42-interacting protein 4 promotes breast cancer cell invasion and formation of invadopodia through activation of N-WASp. *Cancer Res.* **70**, 8347-8356.
Rivero, S., Cardenas, J., Bornens, M. and Rios, R. M. (2009). Microtubule nucleation at the cis-side of the Golgi apparatus requires AKAP450 and GM130. *EMBO J.* **28**, 1016-1028.
Roberts-Galbraith, R. H. and Gould, K. L. (2010). Setting the F-BAR: functions and regulation of the F-BAR protein family. *Cell Cycle* **9**, 4091-4097.
Robles-Valero, J., Martín-Cófreces, N. B., Lamana, A., Macdonald, S., Volkov, Y. and Sánchez-Madrid, F. (2010). Integrin and CD3/TCR activation are regulated by the scaffold protein AKAP450. *Blood* **115**, 4174-4184.
Rolland, Y., Marighetti, P., Malinverno, C., Confalonieri, S., Luise, C., Ducano, N., Palamidessi, A., Bisi, S., Kajiho, H., Troglio, F. et al. (2014). The CDC42-interacting protein 4 controls epithelial cell cohesion and tumor dissemination. *Dev. Cell* **30**, 553-568.
Saengsawang, W., Mitok, K., Viesselmann, C., Pietila, L., Lumbard, D. C., Corey, S. J. and Dent, E. W. (2012). The F-BAR protein CIP4 inhibits neurite formation by producing lamellipodial protrusions. *Curr. Biol.* **22**, 494-501.
Schmidt, P. H., Dransfield, D. T., Claudio, J. O., Hawley, R. G., Trotter, K. W., Milgram, S. L. and Goldenring, J. R. (1999). AKAP350, a multiply spliced protein kinase A-anchoring protein associated with centrosomes. *J. Biol. Chem.* **274**, 3055-3066.
Shanks, R. A., Steadman, B. T., Schmidt, P. H. and Goldenring, J. R. (2002). AKAP350 at the Golgi apparatus: I. Identification of a distinct Golgi apparatus targeting motif in AKAP350. *J. Biol. Chem.* **277**, 40967-40972.
Sutterlin, C. and Colanzi, A. (2010). The Golgi and the centrosome: building a functional partnership. *J. Cell Biol.* **188**, 621-628.
Takahashi, M., Yamagiwa, A., Nishimura, T., Mukai, H. and Ono, Y. (2002). Centrosomal proteins CG-NAP and kendrin provide microtubule nucleation sites by anchoring gamma-tubulin ring complex. *Mol. Biol. Cell* **13**, 3235-3245.
Tang, N. and Marshall, W. F. (2012). Centrosome positioning in vertebrate development. *J. Cell Sci.* **125**, 4951-4961.
Tian, L., Nelson, D. L. and Stewart, D. M. (2000). Cdc42-interacting protein 4 mediates binding of the Wiskott-Aldrich syndrome protein to microtubules. *J. Biol. Chem.* **275**, 7854-7861.
Trinkaus, J. P. (1984). *Cells into Organs: The Forces that Shape the Embryo*, 2nd edn. Englewood Cliffs, NJ: Prentice-Hall.
Truesdell, P., Ahn, J., Chander, H., Meens, J., Watt, K., Yang, X. and Craig, A. W. B. (2014). CIP4 promotes lung adenocarcinoma metastasis and is associated with poor prognosis. *Oncogene* **34**, 3527-3535.
Tsujita, K., Suetsugu, S., Sasaki, N., Furutani, M., Oikawa, T. and Takenawa, T. (2006). Coordination between the actin cytoskeleton and membrane deformation by a novel membrane tubulation domain of PCH proteins is involved in endocytosis. *J. Cell Biol.* **172**, 269-279.
Tzima, E., Kiosses, W. B., del Pozo, M. A. and Schwartz, M. A. (2003). Localized cdc42 activation, detected using a novel assay, mediates microtubule organizing center positioning in endothelial cells in response to fluid shear stress. *J. Biol. Chem.* **278**, 31020-31023.
Vinogradova, T., Paul, R., Grimaldi, A. D., Loncarek, J., Miller, P. M., Yampolsky, D., Magidson, V., Khodjakov, A., Mogilner, A. and Kaverina, I. (2012). Concerted effort of centrosomal and Golgi-derived microtubules is required for proper Golgi complex assembly but not for maintenance. *Mol. Biol. Cell* **23**, 820-833.
Yadav, S., Puri, S. and Linstedt, A. D. (2009). A primary role for Golgi positioning in directed secretion, cell polarity, and wound healing. *Mol. Biol. Cell.* **20**, 1728-1736.
Zhang, J., Bi, M., Zhong, F., Jiao, X., Zhang, D. and Dong, Q. (2013). Role of CIP4 in high glucose induced epithelial–mesenchymal transition of rat peritoneal mesothelial cells. *Ren. Fail.* **35**, 989-995.